Study of radiation damage in ODS steels by positron annihilation spectroscopy

I Bartošová[1,2], A Bouhaddane[1], M Dománková[3], V Slugeň[1], D Wall[4] and F A Selim[2]

[1] Institute of Nuclear and Physical Engineering, Slovak University of Technology in Bratislava, Ilkovičova 3, 812 19 Bratislava, Slovak Republic
[2] Department of Physics, Bowling Green State University, 104 Overman Hall, OH 43403, USA
[3] Department of Materials Science, Faculty of Materials Science and Technology in Trnava, Slovak University of Technology in Bratislava, Paulínska 16, 917 24 Trnava, Slovak Republic
[4] Nuclear Radiation Center, PO Box 641300, Washington State University, Pullman, WA 99164-1300, *USA*

E-mail: iveta.bartosova@stuba.sk

Abstract. Microstructure of various oxide-dispersion-strengthened (ODS) steels with 15% chromium content was studied in term of vacancy defects presence and their accumulation after defined irradiation treatment, respectively. Studied materials originated from Kyoto University and studied via IAEA collaborative project. Samples were characterized "as received" by positron annihilation lifetime spectroscopy and their microstructure was examined by transmission electron microscopy as well. Samples were afterwards irradiated in Washington State University Nuclear Radiation Center via a strong gamma source (6TBq). Damage induced by gamma irradiation was evaluated by positron lifetime measurements in emphasis on defect accumulation in the materials. We have demonstrated strong defect production induced by gamma irradiation which results from positron measurement data.

1. Introduction

Oxide dispersion strengthened steels (ODS) have been developed mainly for high temperature applications for advanced fusion reactor blanket components as well as the next generation fission reactor fuel cladding [1]. The microstructure of these steels is enhanced by dispersed particles of Y_2O_3 which influence dislocation movement and also serve as trapping sites for positrons due to high positron affinity of yttrium. Therefore investigation by means of positron annihilation lifetime spectroscopy (PALS) provides a wide range of information. Positron measurements are supported by transmission electron microscopy (TEM) which provides visual evaluation and overall parameters of the samples.

It is our understanding that the behaviour of ODS steels after gamma irradiation was not yet investigated. Traditionally gamma rays are utilized for food sterilization or irradiation of polymers and are not often utilized for material research of steels because only a really strong source and sufficient

irradiation time can disrupt steel lattice in an extent that we can observe. This approach is therefore somewhat unexplored.

In the area of steel research gamma irradiation is mainly utilized to investigate its effect on the kinetics of carbon steels corrosion [2, 3] or for the production of corrosion related passive films on stainless steels, which present better behaviour and mechanical properties in comparison to un-irradiated samples [4] and provides a new insight into the role of competing oxide film kinetics [5]. There have been also some theoretical studies of gamma irradiation effect on the properties of ferritic reactor pressure vessel (RPV) steels. In [6] they employ MCBEND code to calculate gamma fluxes and energetic gamma ray displacement cross-sections calculated using either Baumann or Alexander methods. They also mention the mechanisms of gamma induced radiation damage of RPV steels. Also estimations of dpa cross sections have been done in Fe by several authors. In the work of Piñera et al. [7] several calculated estimates of dpa cross sections as a function of gamma ray energy of various research groups are compared. However vital data describing concrete gamma irradiation induced defect measurements are absent. We believe that gamma irradiation could be quite beneficial in comparison to other forms of irradiation. Our main concern with traditional neutron irradiation is the activity of the samples. Since we want to investigate the samples by PALS, the activated parasite cobalt peaks would interfere with the start signal of PALS equipment and therefore present false annihilation counts. Deconvolution of the spectra is possible, however quite high errors can be brought into the result. Also a 3-detector system can solve the problem with cobalt. On the other hand long measurement time and also the financial aspect seem as a draw-back. Also handling and waiting for the samples to cool down represents a significant problem. Therefore this novel approach could become an alternative to the traditional neutron irradiation.

Damage production by gamma rays has received less attention than damage by neutrons. Gamma rays create damage through creating fast electrons and it is by this interaction of electrons with atoms in the lattice that damage is produced. A ^{60}Co source emits two gamma rays of 1.17 and 1.33MeV. The main mechanism by which gamma rays of our range of energies induce damage is Compton scattering. Also photoelectric effect can contribute to damage formation. We calculated the maximum kinetic energy of the recoil atom, therefore achieving an elastic collision in a 180° angle, using equation 1 [8].

$$T_m = 2E(E + 2mc^2) * (Mc^2)^{-1} \quad (1)$$

E is the electron kinetic energy, mc^2 is the electron rest energy, M is the iron atom mass.

A displacement energy of 25-40eV is required for displacing an iron atom from the lattice. Literature states that electrons with energies above ≈0.4–0.7MeV (depending on crystallographic direction) will transfer sufficient energies to displace lattice atoms in iron [6]. For energies greater than ≈0.6 MeV, the maximum electron energy approaches the original gamma energy minus ≈0.25 MeV (in our case 0.92 and 1.08MeV). Solving equation 1 a maximum kinetic energy of about 68.5-87eV for the 1.17 and 1.33MeV energies was obtained; therefore applied gamma source is able to induce defects via production of fast electrons.

The aim of this work is to describe microstructural changes in materials lattice after gamma bombardment and determine the resistance of these ODS steels. We predict higher positron trapping due to higher concentration of defects caused by displacements in the lattice.

2. Experimental

2.1. TEM results

Three 15 wt%Cr ODS steels were delivered in form of cylinders. Heat treatment involved hot extrusion at 1150°C and subsequent air cooling. Cylinders were cut into smaller pieces using a band saw. The samples were then polished to high surface reflectance and ready for positron measurements.

For TEM further sample preparation was needed. Thin steel foil with thickness of 0.1mm was prepared by mechanical grinding. Afterwards targets with 3mm diameter were further thinned in Tenupol 5 device in a solution of: 300 ml HNO_3 + 700 ml CH_3OH, voltage 15V and electrolyte temperature 0°C. After cleansing in ethanol and drying, the sample was prepared for TEM. Investigations by TEM were carried out on JEOL 200CX electron microscope with accelerating voltage 200keV. Selected area electron diffraction (SAD) for identification of lattice parameters supplemented TEM analyses. Chemical composition of studied samples is summarized in table 1.

Figure 1 shows TEM observations of sample KOC5-3. The microstructure of all samples is very similar. The figure shows presence of polyhedric ferritic grains with relatively homogenic size. The mean size of ferritic grains for samples 4-3, 5-3 and 6-3 is d_{str} = 550±25 nm, d_{str} = 800±100 nm and d_{str}=650±40 nm, respectively. We also observed in figure 2 small globular particles, which show strong heterogeneity whether in size or distribution. Particle size varied from 2-300 nm however in all samples more than 60% of particles were 20-40 nm in diameter. SAD identified these particles to be Y_2O_3. Interestingly in sample 5-3 the Y_2O_3 phase was found in two modifications- bcc and also fcc. Also a presence of quasi globular particles was acknowledged in samples KOC4-3 and KOC5-3 which precipitate mainly on ferritic grain boundaries. Due to chemical composition and SAD results we believe the secondary phase is that of $M_{23}C_6$. Analyses also provided some evidence of precipitations interacting with Y_2O_3 particles at grain boundaries and dislocations as can be seen in figures 3 and 4.

Table 1. Chemical composition of studied steels KOC4-3, 5-3 and 6-3.

	KOC4-3	KOC5-3	KOC6-3
C	0.027	0.031	0.028
Si	0.03	0.03	0.03
Mn	0.02	0.02	0.01
P	0.005	0.005	0.005
S	0.002	0.002	0.002
Cr	15.33	15.15	15.41
W	1.9	1.9	1.8
Al	3.8	3.9	3.87
Ti	0.12	0.11	0.12
Y	0.26	0.26	0.26
O	0.14	0.14	0.14
N	0.009	0.005	0.007
Ar	0.006	0.005	0.005
Zr	0.32	0.58	-
Hf	-	-	0.59
Y_2O_3	0.33	0.33	0.33

From figure 4 it seems that small Y_2O_3 are localized in grain boundaries, which is appropriate since grain boundaries act as sinks. It is possible that they became localized during fabrication since hot extrusion at 1150°C and subsequent air cooling are part of the fabrication process. The area adjacent to the grain boundary seems relatively Y_2O_3 particle free. Y_2O_3 distort the surrounding crystal lattice which results in dislocation formation.

Positron annihilation lifetime spectroscopy was applied on as- received samples and after gamma irradiation. Positron lifetime measurements were carried out using ^{22}Na, with activity about 20μCi, deposited on a kapton foil. The source was sandwiched between two identical samples of steel. A minimum of $1.3x10^6$ counts was collected for each of the three runs conducted for individual samples. Positron lifetime data was evaluated using PATFIT-88 software. A detailed description of the

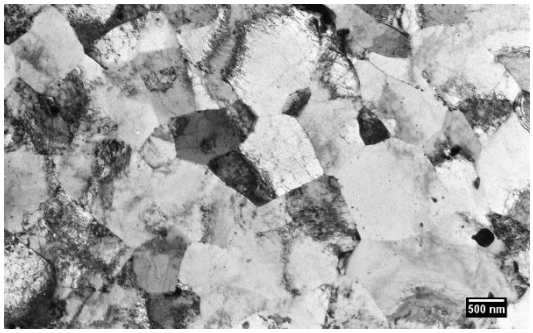

Figure 1. Bright field TEM image of sample KOC 5-3 in as- received state. Microstructure contains polyedric ferritic grains.

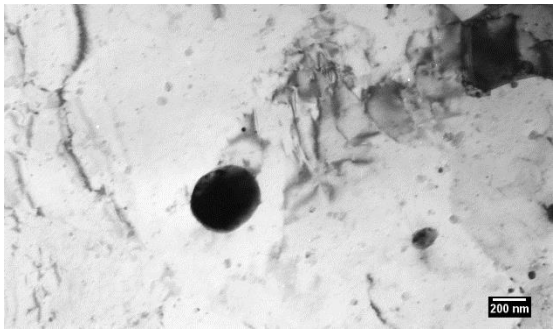

Figure 2. Detail on globular particle identified as Y_2O_3 in KOC4-3.

Figure 3. Interaction of dislocations with precipitates in KOC6-3.

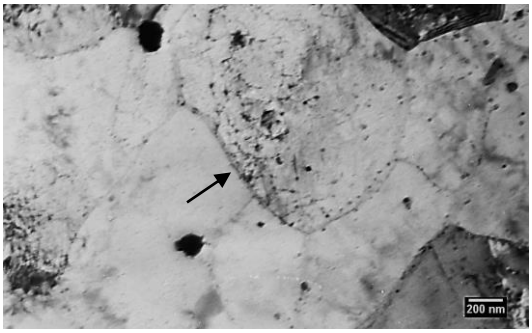

Figure 4. Area with low density of globular particles in ferritic matrix in KOC6-3. On the ferritic grain we can observe entrapment of dislocations around Y_2O_3 particles depicted by the arrow.

resolution function required for spectrum analysis used three Gaussian functions with intensities 80%, 10%, 10%, and appropriate relative shifts. The lifetime spectrum is analyzed as a sum of exponential decay components, convoluted with the Gaussians functions describing the spectrometer timing resolution using POSITRONFIT. Decay components due to annihilation in NaCl (≈430ps) and kapton foil (≈382ps) were subtracted in the procedure.

2.2. Irradiation details

Samples were irradiated at the Washington State University Nuclear Radiation Center using gamma rays generated by a ^{60}Co source. The ^{60}Co irradiator consists of a rod of radioactive Co metal which is stored in a pool of water at a depth of 7.6 meters. The ^{60}Co source material is adjacent to a 15 cm diameter aluminum tube which extends from above the surface of the pool down to the ^{60}Co source. The aluminum tube is sealed on the end which is at the bottom of the storage pool and is open to the atmosphere above the surface of the pool water; this allows samples to be placed in a basket to be lowered down into the aluminum tube and positioned adjacent to the ^{60}Co without having to immerse the samples in the storage pool water. The activity of the ^{60}Co source was 6.09 TBq and the irradiation was conducted continuously for 1742 hours. The distance from the ^{60}Co to the ODS samples was 9 cm. Sample temperatures were held at 30 ± 5° C during the irradiation.

3. Results

Figure 5 and 6 represent the results obtained from positron annihilation lifetime spectroscopy. The data was fitted by three exponential components where only the first two are interesting in

characterization of studied materials. These lifetimes LT_1, LT_2 are shown in figure 5 and their relative intensities in figure 6. The average lifetime value was calculated using equation (2).

$$LT_{avg} = LT_1 I_1 + LT_2 I_2 \quad (2)$$

It is logical to assume that the shorter component LT_1 arises from annihilations of delocalized positrons. The longer component LT_2 represents contribution of the positrons trapped at one or more types of defects. The second component LT_2 for all the samples in as-received state is in the range 197-217 ps. This range corresponds to di-vacancies and suggests that positrons most likely get trapped and annihilate at defects of the same kind in all samples. The concentration of these defects in samples KOC4-3 and 5-3 is 55, 57% respectively; however in KOC6-3 the concentration is about 42% and I1 is much higher in comparison to materials KOC4-3, 5-3. Sample KOC6-3 contains much less defects in base state then the previous. By TEM technique we also asserted that small defects like dislocations are present in the samples.

It is generally believed that the dislocation line represents only a shallow positron trap. The positron diffuses until it finds a vacancy attached to the dislocation, where it afterwards annihilates. From TEM we saw that dislocations get trapped around Y_2O_3. Therefore we believe that the positron diffuses to a di-vacancy (from LT_2 value) attached to the dislocation which is surrounded by Y_2O_3 particles. The reduced positron lifetime LT_1 moves around 83-100ps and is in strong relation with LT_2 due to the fitting approach. The average lifetime in all samples is around 147±1ps before gamma irradiation.

After gamma irradiation we can observe major change in positron lifetime. Both lifetimes increased significantly. Lifetime LT_2 indicates formation of large clusters of vacancies in KOC4-3, 5-3 and vacancy clusters of about 4 vacancies in KOC6-3. The intensities also drastically shifted. After gamma irradiation I_2 decreased below 30% in all cases. Intensity I1 on the other hand increased above 70%. This indicates that gamma irradiation formed larger defects but with smaller intensity. Di-vacancies merged into larger defects forming vacancy clusters. Again, sample KOC6-3 seems to have fewer defects and is therefore more immune to gamma irradiation. The main difference in this steel is almost

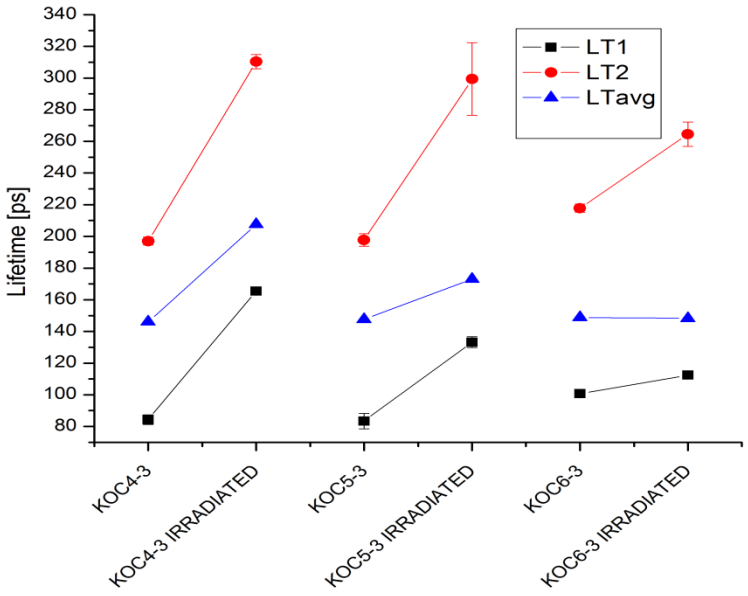

Figure 5. Reduced lifetime in bulk (LT_1) and in defects (LT_2). Average lifetime (LT_{avg}) was calculated.

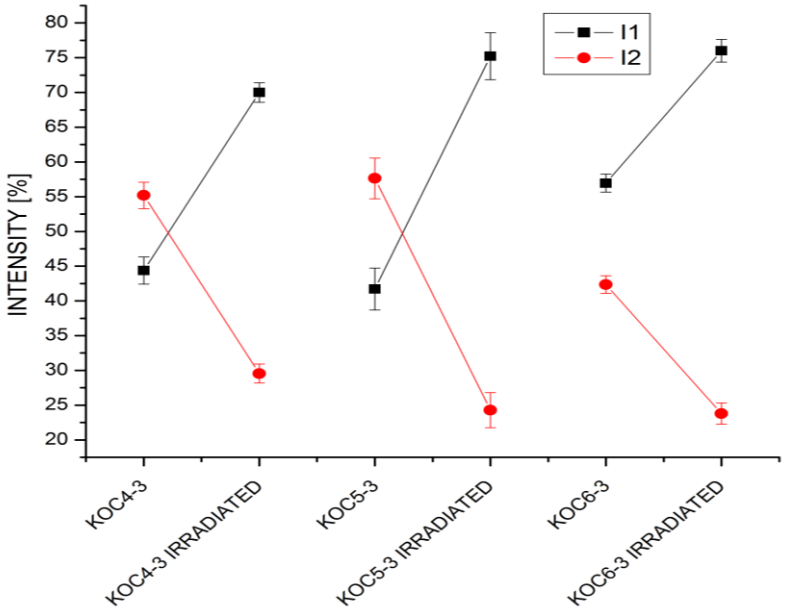

Figure 6. Intensities of particular lifetime components. Intensity I_1, I_2 corresponds to LT_1 and LT_2 respectively.

0.6 wt% content of hafnium and no zirconium additions. In [9] they implanted hafnium ions into foils of 9 wt%Cr ferritic steels to study the effect of hafnium on the grain boundary precipitation kinetics. It was found that the implantation of hafnium into the steel completely prohibited the formation of the common grain boundary $M_{23}C_6$ particles. In our case we can assume similar behaviour. Instead of $M_{23}C_6$ carbides hafnium forms MX type precipitates which increase the concentration of chromium in the matrix and is expected to improve the intergranular corrosion resistance of the material [10]. We do not state that all $M_{23}C_6$ formation was denied by hafnium, however we believe that hafnium plays a significant role in precipitation kinetics.

4. Conclusion

Three steels with different chemical content were investigated by transmission electron microscopy and positron annihilation spectroscopy. Samples designated KOC4-3 and KOC5-3 seem to have very similar properties as to defect type and concentration. Third sample KOC6-3 which is the only sample lacking zirconium and containing hafnium instead shows different behaviour as to initial microstructure and irradiation resistance after gamma irradiation. We attribute this improved resistance to hafnium which to some extent prohibits formation of $M_{23}C_6$ and forms hafnium carbides that have beneficial effect on the irradiation resistance.

We demonstrated a novel approach how to induce and investigate defects in steels. A high gamma irradiation source and appropriate irradiation time has proven to be sufficient by inducing major defects to the microstructure. Gamma irradiation does not interfere with positron measurements or TEM by undesirable side effects like in the case of neutron irradiation. In our future work we will also compare neutron irradiation and gamma irradiation on these samples. Nevertheless we believe that gamma irradiation of steels could be a helpful defect inducing method lacking the disadvantages of classical neutron irradiation.

References

[1] Kasada R, Lee S G, Isselin J, Lee J H, Omura T, Kimura A, Okuda T, Inoue M, Ukai S, Ohnuki S, Fujisawa T, Abe F 2011 *J.Nucl.Mat.* **417** 180

[2] Fujita N, Matsuura CH, Kazuhiko S 2000 *Rad. Phys. and Chem.* **58** 139
[3] Daub K, Zhang X, Noel J J, Wren J C 2011 *Corrosion Science* **53** 11
[4] Capobianco G, Sandona G, Monetta T, Bellucci F 1993 *Corrosion Science* **35** 35
[5] Knapp Q W, Wren J C 2012 *Electrochimica Acta* **80** 90
[6] Knott J F, English C A, Weaver D R, Lidbury D P G 2005 *Inter. J. Press. Vess. and Pip.* **82** 929
[7] Piñera I, Cruz C M, Leyva A, Abreu Y, Cabal A E, Espen P V, Remortel N V 2014 *Nucl. Instr. and Meth. in Phys. Research* B **339** 1
[8] Piñera I, Cruz C M, Leyva A, Abreu Y 2007 *Nucleus*, **41** 39
[9] Yin Y F, Faulkner R G 2005 *Mat. Sc. and Tech.* **21** 1239
[10] Kim J K, Kim Y H, Lee J S, Kim K Y 2010 *Corr. Sc.* **52** 1847